

The Standard Model of Particle Physics: Status & Low-Energy Tests

Antonio Pich

IFIC, Universitat de València – CSIC, Apt. 22085, E-46071 València, Spain

Abstract. Precision measurements of low-energy observables provide stringent tests of the Standard Model structure and accurate determinations of its parameters. An overview of the present experimental status is presented. The main topics discussed are the muon anomalous magnetic moment, the asymptotic freedom of strong interactions, the lepton universality of gauge couplings, the quark flavour structure and CP violation.

1 Standard Model Structure

The Standard Model (SM) [1,2] is a gauge theory, based on the group $SU(3)_C \otimes SU(2)_L \otimes U(1)_Y$, which describes strong, weak and electromagnetic interactions, via the exchange of the corresponding spin-1 gauge fields: 8 massless gluons and 1 massless photon for the strong and electromagnetic forces, respectively, and 3 massive bosons, W^\pm and Z , for the weak interaction. The gauge symmetry determines the dynamics in terms of the three couplings g_s , g and g' , associated with the $SU(3)_C$, $SU(2)_L$ and $U(1)_Y$ subgroups. Strong interactions are governed by the first group factor, while the other two provide a unified description of the electroweak forces, their gauge parameters being related through $g \sin \theta_W = g' \cos \theta_W = e$.

The fermionic matter content is given by the known leptons and quarks, which are organized in a 3-fold family structure:

$$\begin{bmatrix} \nu_e & u \\ e^- & d' \end{bmatrix}, \quad \begin{bmatrix} \nu_\mu & c \\ \mu^- & s' \end{bmatrix}, \quad \begin{bmatrix} \nu_\tau & t \\ \tau^- & b' \end{bmatrix}, \quad (1)$$

where (each quark appears in 3 different *colours*)

$$\begin{bmatrix} \nu_l & q_u \\ l^- & q_d \end{bmatrix} \equiv \begin{pmatrix} \nu_l \\ l^- \end{pmatrix}_L, \quad \begin{pmatrix} q_u \\ q_d \end{pmatrix}_L, \quad l^-_R, \quad (q_u)_R, \quad (q_d)_R, \quad (2)$$

plus the corresponding antiparticles. Thus, the left-handed fields are $SU(2)_L$ doublets, while their right-handed partners transform as $SU(2)_L$ singlets. The three fermionic families in (1) appear to have identical properties (gauge interactions); they only differ by their mass and their flavour quantum number.

The gauge symmetry is broken by the vacuum, which triggers the Spontaneous Symmetry Breaking (SSB) of the electroweak group to the electromagnetic subgroup:

$$SU(3)_C \otimes SU(2)_L \otimes U(1)_Y \xrightarrow{\text{SSB}} SU(3)_C \otimes U(1)_{QED}. \quad (3)$$

Invited talk at the ESO–CERN–ESA Symposium on Astronomy, Cosmology and Fundamental Physics (Garching bei München, Germany, March 2002)

The SSB mechanism generates the masses of the weak gauge bosons, and gives rise to the appearance of a physical scalar particle, the so-called *Higgs*. The fermion masses and mixings are also generated through the SSB mechanism.

The SM constitutes one of the most successful achievements in modern physics. It provides a very elegant theoretical framework, which is able to describe all known experimental facts in particle physics. A detailed description of the SM and its impressive phenomenological success can be found in [3,4].

2 Quantum Corrections

The high accuracy achieved by the most recent experiments allows to make stringent tests of the SM structure at the level of quantum corrections. The following discussion concentrates on Quantum Electrodynamics (QED) and Quantum Chromodynamics (QCD). Electroweak effects are covered in [5].

2.1 Running Couplings

Let us consider the electromagnetic interaction between two electrons. At lowest order, the scattering amplitude $T(q^2) \sim \alpha/q^2$ with $\alpha = e^2/(4\pi)$. The leading quantum corrections are generated by the photon self-energy contribution:

$$T(Q^2) \sim \frac{\alpha}{Q^2} \{1 - \Pi(Q^2) + \Pi(Q^2)^2 + \dots\} = \frac{\alpha}{Q^2} \frac{1}{1 + \Pi(Q^2)} \sim \frac{\alpha(Q^2)}{Q^2}.$$

This defines an effective *running* coupling,

$$\alpha(Q^2) = \frac{\alpha(Q_0^2)}{1 - \frac{\beta_1}{2\pi} \alpha(Q_0^2) \ln(Q^2/Q_0^2)}, \quad (4)$$

where $Q^2 \equiv -q^2$ and $\alpha(m_e^2) = \alpha$. The e^+e^- loop induces a logarithmic correction with $\beta_1 = 2/3 > 0$. Therefore, the effective QED running coupling increases with the energy scale: $\alpha(Q^2) > \alpha(Q_0^2)$ if $Q^2 > Q_0^2$, i.e., the electromagnetic charge decreases at large distances. This can be intuitively understood as the screening due to virtual e^+e^- pairs generated, through quantum effects, around the electron charge. The physical QED vacuum behaves as a polarized dielectric

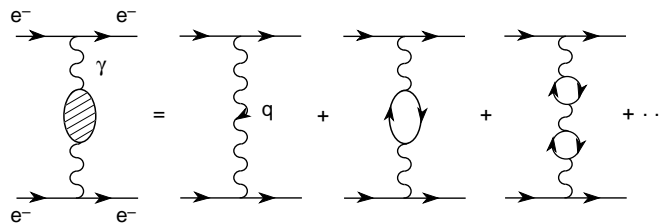


Fig. 1. Photon self-energy contribution to e^-e^- scattering

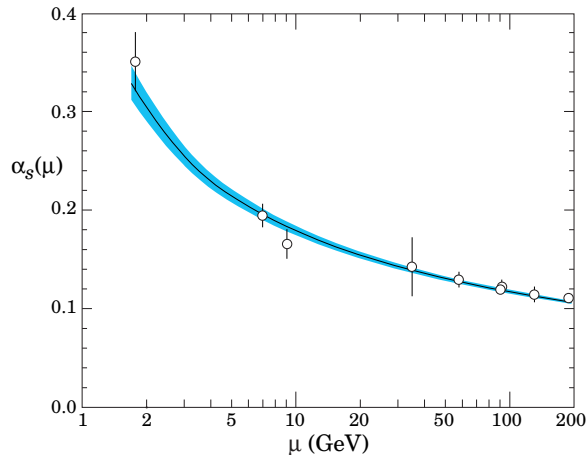


Fig. 2. Energy dependence [10] of the strong coupling α_s

medium. The huge difference between the electron and Z mass scales makes this quantum correction relevant at LEP energies [6,7]:

$$\alpha(m_e^2)^{-1} = 137.03599976(50) > \alpha(M_Z^2)^{-1} = 128.95 \pm 0.05. \quad (5)$$

The strong interaction between two quarks can be analyzed in a similar way. Owing to the non-abelian character of the $SU(3)_C$ group, QCD leads to cubic and quartic self-interactions among gluons. This results in a strong running coupling $\alpha_s(Q^2)$ with the same Q^2 dependence (4), but with a negative β_1 [8]:

$$\beta_1 = \frac{2N_f - 11N_C}{6} < 0. \quad (6)$$

The contribution proportional to the number of quark flavours N_f is generated by the $q\bar{q}$ loop corrections to the gluon self-energy. The gluonic self-interactions introduce the additional negative term proportional to the number of quark colours N_C . Since $\beta_1 < 0$, $\alpha_s(Q^2)$ decreases at short distances. Thus, QCD has the required property of *asymptotic freedom*: quarks behave as free particles when $Q^2 \rightarrow \infty$. The predicted running of α_s , known to four loops [9], agrees very well with the experimental determinations at different energies. Normalizing all measurements at the Z mass scale, the present world average is [10]:

$$\alpha_s(M_Z^2) = 0.118 \pm 0.002. \quad (7)$$

2.2 Lepton Anomalous Magnetic Moments

The most stringent QED test [11,12] comes from the high-precision measurements of the e [10] and μ [13] anomalous magnetic moments $a_l^\gamma \equiv (g_l - 2)/2$:

$$a_e^\gamma = \begin{cases} (115\,965\,215.35 \pm 2.40) \times 10^{-11} & \text{(Theory)} \\ (115\,965\,218.69 \pm 0.41) \times 10^{-11} & \text{(Experiment)} \end{cases}, \quad (8a)$$

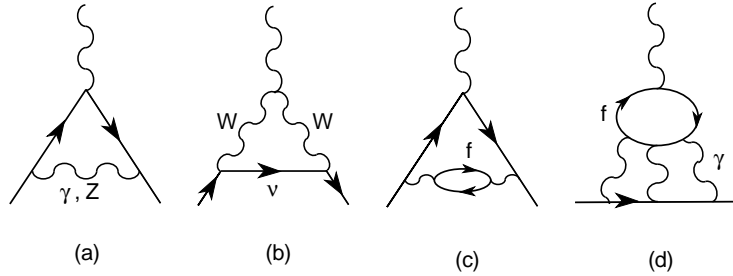


Fig. 3. Some Feynman diagrams contributing to a_l^γ

$$a_\mu^\gamma = \begin{cases} (1\,165\,917.9 \pm 1.0) \times 10^{-9} & \text{(Theory)} \\ (1\,165\,920.3 \pm 1.5) \times 10^{-9} & \text{(Experiment)} \end{cases} . \quad (8b)$$

The impressive agreement between theory and experiment promotes QED to the level of the best theory ever build by the human mind to describe nature.

To a measurable level, a_e^γ arises entirely from virtual electrons and photons; these contributions are known [11] to $O(\alpha^4)$. The theoretical error is dominated by the uncertainty in the input value of the QED coupling α . Turning things around, a_e^γ provides the most precise determination of the fine structure constant.

The anomalous magnetic moment of the muon is sensitive to virtual contributions from heavier states; compared to a_e^γ , they scale as m_μ^2/m_e^2 . The main theoretical uncertainty on a_μ^γ has a QCD origin. Since quarks have electric charge, virtual quark-antiquark pairs induce *hadronic vacuum polarization* corrections to the photon propagator (Fig. 3.c). Owing to the non-perturbative character of QCD at low energies, the light-quark contribution cannot be reliably calculated at present; fortunately, this effect can be extracted from the measurement of the cross-section $\sigma(e^+e^- \rightarrow \text{hadrons})$ and from the invariant-mass distribution of the final hadrons in τ decays [6]. Additional QCD uncertainties stem from the smaller *light-by-light scattering* contributions (Fig. 3.d); a recent reevaluation of these corrections [14] has detected a sign mistake in previous calculations [15], improving the agreement with the experimental measurement [13].

The Brookhaven E821 experiment [13] is expected to push its sensitivity to at least 4×10^{-10} , and thereby observe the contributions from virtual W^\pm and Z bosons [12,16]. This would require a better control of the QCD corrections.

3 Lepton Universality

In the SM all lepton doublets have identical couplings to the W boson:

$$\mathcal{L} = \frac{g}{2\sqrt{2}} W_\mu^\dagger \sum_l \bar{\nu}_l \gamma^\mu (1 - \gamma_5) l + \text{h.c.} \quad (l = e, \mu, \tau) . \quad (9)$$

Comparing the measured decay widths of leptonic or semileptonic decays which

Table 1. Experimental determinations of the ratios g_l/g_V

	$\Gamma_{\tau \rightarrow \nu_\tau \mu \bar{\nu}_\mu} / \Gamma_{\nu_\tau e \bar{\nu}_e}$	$\Gamma_{\pi \rightarrow \mu \bar{\nu}_\mu} / \Gamma_{\pi \rightarrow e \bar{\nu}_e}$	$\Gamma_{W \rightarrow \mu \bar{\nu}_\mu} / \Gamma_{W \rightarrow e \bar{\nu}_e}$
$ g_\mu/g_e =$	1.0006 ± 0.0021	1.0017 ± 0.0015	1.000 ± 0.011

	$\Gamma_{\tau \rightarrow \nu_\tau e \bar{\nu}_e} / \Gamma_{\mu \rightarrow \nu_\mu e \bar{\nu}_e}$	$\Gamma_{\tau \rightarrow \nu_\tau \pi} / \Gamma_{\pi \rightarrow \mu \bar{\nu}_\mu}$	$\Gamma_{\tau \rightarrow \nu_\tau K} / \Gamma_{K \rightarrow \mu \bar{\nu}_\mu}$	$\Gamma_{W \rightarrow \tau \bar{\nu}_\tau} / \Gamma_{W \rightarrow \mu \bar{\nu}_\mu}$
$ g_\tau/g_\mu =$	0.9995 ± 0.0023	1.005 ± 0.007	0.977 ± 0.016	1.026 ± 0.014

	$\Gamma_{\tau \rightarrow \nu_\tau \mu \bar{\nu}_\mu} / \Gamma_{\mu \rightarrow \nu_\mu e \bar{\nu}_e}$	$\Gamma_{W \rightarrow \tau \bar{\nu}_\tau} / \Gamma_{W \rightarrow e \bar{\nu}_e}$
$ g_\tau/g_e =$	1.0001 ± 0.0023	1.026 ± 0.014

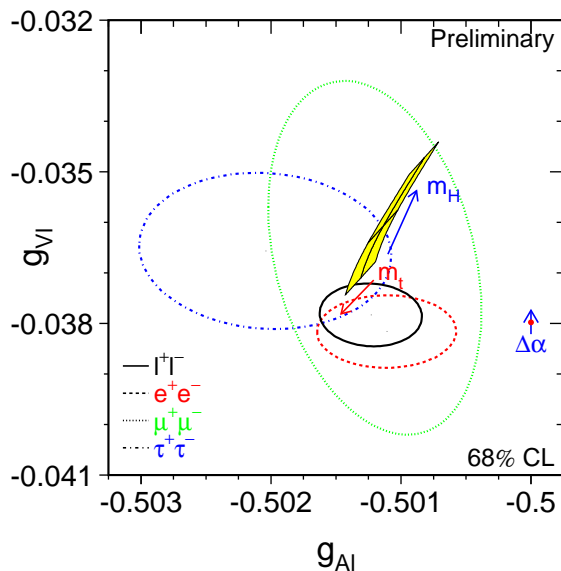


Fig. 4. Contours of 68% probability in the a_l - v_l plane from LEP and SLD measurements [17]. The solid contour assumes lepton universality. The shaded region corresponds to the SM prediction for $m_t = 174.3 \pm 5.1$ GeV and $m_H = 300^{+700}_{-186}$ GeV.

only differ by the lepton flavour, one can test experimentally that the W interaction is indeed the same, i.e. that $g_e = g_\mu = g_\tau \equiv g$. As shown in Table 1, the present data [4,10,17] verify the universality of the leptonic charged-current couplings to the 0.2% level.

The interactions of the neutral Z boson are diagonal in flavour. Moreover, all fermions with equal electric charge have identical axial-vector, $a_f = T_3^f = \pm 1/2$,

and vector, $v_f = T_3^f (1 - 4 |Q_f| \sin^2 \theta_W)$, couplings to the Z . This has been accurately tested at LEP and SLD through a precise analysis of $e^+e^- \rightarrow \gamma, Z \rightarrow f\bar{f}$ data. Figure 4 shows the 68% probability contours in the a_l - v_l plane, obtained from leptonic observables [17]. The universality of the leptonic Z couplings is now verified to the 0.15% level for a_l , while only a few per cent precision has been achieved for v_l due to the smallness of the leptonic vector coupling. The measured leptonic asymmetries provide an accurate determination of the electroweak mixing angle [17]:

$$\sin^2 \theta_W = 0.23113 \pm 0.00021 . \quad (10)$$

4 Flavour Mixing

In the SM, all mass scales are generated through the Higgs mechanism. After the SSB, the Yukawa couplings to the Higgs scalar doublet give rise to non-diagonal fermionic mass terms. The mass eigenstates are then different from the weak eigenstates, which leads to flavour mixing in the charged-current interaction:

$$\mathcal{L} = \frac{g}{2\sqrt{2}} W_\mu^\dagger \sum_{ij} \bar{u}_i \gamma^\mu (1 - \gamma_5) \mathbf{V}_{ij} d_j + \text{h.c.} . \quad (11)$$

With non-zero neutrino masses, there are analogous mixing effects in the lepton sector, which are covered in [18].

The Cabibbo-Kobayashi-Maskawa [19,20] (CKM) matrix \mathbf{V} is unitary and couples any up-type quark with all down-type quarks. It is a priori unknown, because the gauge symmetry does not fix the Yukawa couplings. The matrix element \mathbf{V}_{ij} can be obtained experimentally from semileptonic weak processes associated with the quark transition $d_j \rightarrow u_i l^- \bar{\nu}_l$. The present determinations are summarized in Table 2. The uncertainties are dominated by theoretical errors, related to the strong interaction which binds quarks into hadrons.

The most precisely known CKM matrix element is \mathbf{V}_{ud} . The weighted average of the two determinations in Table 2 gives $\mathbf{V}_{ud} = 0.9738 \pm 0.0008$. Taking for \mathbf{V}_{us} the more reliable K_{e3} determination, one obtains

$$|\mathbf{V}_{ud}|^2 + |\mathbf{V}_{us}|^2 + |\mathbf{V}_{ub}|^2 = 0.9965 \pm 0.0019 . \quad (12)$$

The unitarity of \mathbf{V}_{ij} appears to be slightly violated by 1.8σ . At this level of precision, a small underestimate of some uncertainties seems plausible. A less accurate unitarity test is provided by the hadronic width of the W boson [17]:

$$\sum_{j=d,s,b} (|\mathbf{V}_{uj}|^2 + |\mathbf{V}_{cj}|^2) = 2.039 \pm 0.025 . \quad (13)$$

The CKM matrix shows a hierarchical pattern, with its diagonal elements being very close to one, the ones connecting the two first generations having a size $\lambda \equiv |\mathbf{V}_{us}|$, the mixing between the second and third families being of order

Table 2. Direct \mathbf{V}_{ij} determinations.

CKM entry	Value	Source
$ \mathbf{V}_{ud} $	0.9740 ± 0.0010	Nuclear β decay [10]
	0.9733 ± 0.0015	$n \rightarrow p e^- \bar{\nu}_e$ [10]
$ \mathbf{V}_{us} $	0.2196 ± 0.0023	K_{e3} [10]
	0.2176 ± 0.0026	Hyperon decays [10]
$ \mathbf{V}_{cd} $	0.224 ± 0.016	$\nu d \rightarrow c X$ [10]
$ \mathbf{V}_{cs} $	1.04 ± 0.16	$D \rightarrow \bar{K} e^+ \nu_e$ [10]
$ \mathbf{V}_{cb} $	0.0421 ± 0.0022	$B \rightarrow D^* l \bar{\nu}_l$ [21]
	0.0404 ± 0.0011	$b \rightarrow c l \bar{\nu}_l$ [21]
$ \mathbf{V}_{ub} $	0.0033 ± 0.0006	$B \rightarrow \rho l \bar{\nu}_l$ [22]
	0.0041 ± 0.0006	$b \rightarrow u l \bar{\nu}_l$ [23,24]
$ \mathbf{V}_{tb} / \sqrt{\sum_q \mathbf{V}_{tq} ^2}$	$0.97^{+0.16}_{-0.12}$	$t \rightarrow b W / q W$ [25]

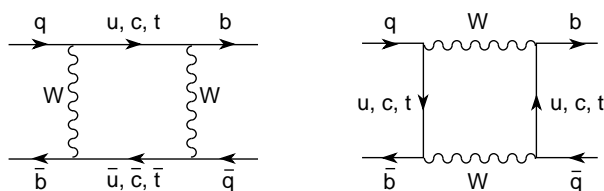
λ^2 , and the mixing between the first and third quark flavours having a much smaller size of about λ^3 . It is convenient to use the parameterization [26]:

$$\mathbf{V} = \begin{bmatrix} 1 - \lambda^2/2 & \lambda & A\lambda^3(\rho - i\eta) \\ -\lambda & 1 - \lambda^2/2 & A\lambda^2 \\ A\lambda^3(1 - \rho - i\eta) & -A\lambda^2 & 1 \end{bmatrix} + O(\lambda^4). \quad (14)$$

Imposing the unitarity constraint, the CKM determinations in Table 2 imply

$$\lambda = 0.223 \pm 0.003, \quad A = 0.83 \pm 0.04, \quad \sqrt{\rho^2 + \eta^2} = 0.40 \pm 0.07. \quad (15)$$

4.1 B^0 - \bar{B}^0 Mixing


Fig. 5. B^0 - \bar{B}^0 mixing diagrams

Additional information on the CKM parameters is obtained from flavour-changing neutral-current transitions, occurring at the 1-loop level. An important

example is provided by the mixing between the B^0 meson and its antiparticle:

$$\langle \bar{B}_d^0 | \mathcal{H}_{\Delta B=2} | B_0 \rangle \sim \left\{ \sum_{ij=u,c,t} \mathbf{V}_{id} \mathbf{V}_{ib}^* \mathbf{V}_{jd}^* \mathbf{V}_{jb} S(r_i, r_j) \right\} \left(\frac{2}{3} M_B^2 \xi_B^2 \right), \quad (16)$$

with $S(r_i, r_j)$ a loop function of $r_i \equiv m_i^2/M_W^2$. Owing to the unitarity of the CKM matrix, the mixing amplitude vanishes for equal (up-type) quark masses. Thus the effect is proportional to the mass splittings between the u , c and t quarks. Since all CKM factors have a similar size, $\mathbf{V}_{ud} \mathbf{V}_{ub}^* \sim \mathbf{V}_{cd} \mathbf{V}_{cb}^* \sim \mathbf{V}_{td} \mathbf{V}_{tb}^* \sim A\lambda^3$, the top contribution dominates completely. This transition can then be used to perform an indirect determination of $|\mathbf{V}_{td}|$. The main uncertainty stems from the hadronic matrix element of the four-quark operator generated by the box diagrams in Fig. 5, which is characterized through the non-perturbative parameter $\xi_B \equiv \sqrt{2\bar{B}_B} f_B = 230 \pm 45$ MeV [27,28]. The measured mixing between the B_d^0 and \bar{B}_d^0 mesons, $\Delta M_{B_d^0} = 0.496 \pm 0.007$ ps $^{-1}$ [23], implies:

$$|\mathbf{V}_{td}| = 0.0077 \pm 0.0011, \quad \sqrt{(1-\varrho)^2 + \eta^2} \approx \left| \frac{\mathbf{V}_{td}}{\lambda \mathbf{V}_{cb}} \right| = 0.84 \pm 0.12. \quad (17)$$

A similar analysis can be applied to the B_s^0 - \bar{B}_s^0 mixing. The non-perturbative uncertainties are reduced to the level of $SU(3)$ breaking through the ratio

$$\frac{\Delta M_{B_s^0}}{\Delta M_{B_d^0}} \approx \frac{M_{B_s^0} \xi_{B_s^0}^2}{M_{B_d^0} \xi_{B_d^0}^2} \left| \frac{\mathbf{V}_{ts}}{\mathbf{V}_{td}} \right|^2 \equiv \Omega^2 \left| \frac{\mathbf{V}_{ts}}{\mathbf{V}_{td}} \right|^2. \quad (18)$$

Taking $\Omega \approx 1.15 \pm 0.08$ [27,28], the experimental bound $\Delta M_{B_s^0} > 14.9$ ps $^{-1}$ (95% CL) [23] implies

$$\left| \frac{\mathbf{V}_{ts}}{\mathbf{V}_{td}} \right| \approx \frac{1}{\lambda \sqrt{(1-\varrho)^2 + \eta^2}} > 4.2. \quad (19)$$

5 CP Violation

With N_G fermion generations, the matrix \mathbf{V} is characterized by $N_G(N_G-1)/2$ moduli and $(N_G-1)(N_G-2)/2$ phases. In the simpler case of two fermion families \mathbf{V} is determined by a single parameter, the so-called Cabibbo angle [19], while for $N_G = 3$ the CKM matrix is described by 3 angles and 1 phase [20]. This is the only complex phase in the SM Lagrangian; thus, it is a unique source for violations of the CP symmetry. It was for this reason that the third generation was assumed to exist [20], before the discovery of the τ and the b .

5.1 Kaon Physics

For many years, the only experimental evidence of CP-violation phenomena came from the kaon system. The ratios,

$$\frac{A(K_L \rightarrow \pi^+ \pi^-)}{A(K_S \rightarrow \pi^+ \pi^-)} \approx \varepsilon_K + \varepsilon'_K, \quad \frac{A(K_L \rightarrow \pi^0 \pi^0)}{A(K_S \rightarrow \pi^0 \pi^0)} \approx \varepsilon_K - 2\varepsilon'_K, \quad (20)$$

involve final 2π states which are even under CP. Therefore, they measure a CP-violating amplitude which can originate either from a small CP-even admixture in the initial K_L state (indirect CP violation), parameterized by ε_K , or from direct CP violation in the decay amplitude. This latter effect, parameterized by ε'_K , requires the interference between the two $K \rightarrow 2\pi$ isospin ($I = 0, 2$) amplitudes, with different weak and strong phases.

The parameter ε_K is well determined [10]:

$$\varepsilon_K = (2.271 \pm 0.017) \times 10^{-3} e^{i\phi(\varepsilon_K)}, \quad \phi(\varepsilon_K) = 43.5^\circ \pm 0.5^\circ. \quad (21)$$

ε_K has been also measured [10,29] through the CP asymmetry between the two $K_L \rightarrow \pi^\mp l^\pm \bar{\nu}_l$ decay widths, which implies $\text{Re}(\varepsilon_K) = (1.654 \pm 0.032) \times 10^{-3}$, in good agreement with (21).

The value of ε'_K has been established very recently. The present experimental world average [30,31,32,33],

$$\text{Re}(\varepsilon'_K/\varepsilon_K) = (1.72 \pm 0.18) \times 10^{-3}, \quad (22)$$

provides clear evidence for the existence of direct CP violation.

The CKM mechanism generates CP-violation effects both in the $\Delta S = 2$ K^0 - \bar{K}^0 transition (box diagrams) and in the $\Delta S = 1$ decay amplitudes (penguin diagrams). The theoretical analysis of K^0 - \bar{K}^0 mixing is quite similar to the one applied to the B system. This time, however, the charm loop contributions are non-negligible. The main uncertainty stems from the calculation of the hadronic matrix element of the four-quark $\Delta S = 2$ operator, which is usually parameterized through the non-perturbative parameter \hat{B}_K .

The experimental value of ε_K specifies a hyperbola in the (ϱ, η) plane. This is shown in Fig. 6 [34], together with the constraints obtained from $|\mathbf{V}_{ub}/\mathbf{V}_{cb}|$, B_d^0 - \bar{B}_d^0 mixing and the experimental bound on $\Delta M_{B_s^0}$. This figure assumes [34] $\hat{B}_K = 0.87 \pm 0.06 \pm 0.13$, $\xi_B = 230 \pm 25 \pm 20$ MeV and $\Omega = 1.15 \pm 0.04 \pm 0.05$.

The theoretical estimate of $\varepsilon'_K/\varepsilon_K$ is more involved [35], because several four-quark operators need to be considered in the analysis. Moreover, the strong rescattering of the final pions generates an important enhancement through infrared logarithms [36]. Taking into account all large logarithmic corrections at short and long distances, the SM prediction for ε'/ε is found to be [36]:

$$\text{Re}(\varepsilon'/\varepsilon) = (1.7 \pm 0.2_{-0.5}^{+0.8} \pm 0.5) \times 10^{-3}, \quad (23)$$

in excellent agreement with the measured experimental value (22).

5.2 B Physics

The unitarity tests in (12) and (13) involve only the moduli of the CKM parameters, while CP violation has to do with their phases. The most interesting off-diagonal unitarity condition is

$$\mathbf{V}_{ub}^* \mathbf{V}_{ud} + \mathbf{V}_{cb}^* \mathbf{V}_{cd} + \mathbf{V}_{tb}^* \mathbf{V}_{td} = 0, \quad (24)$$

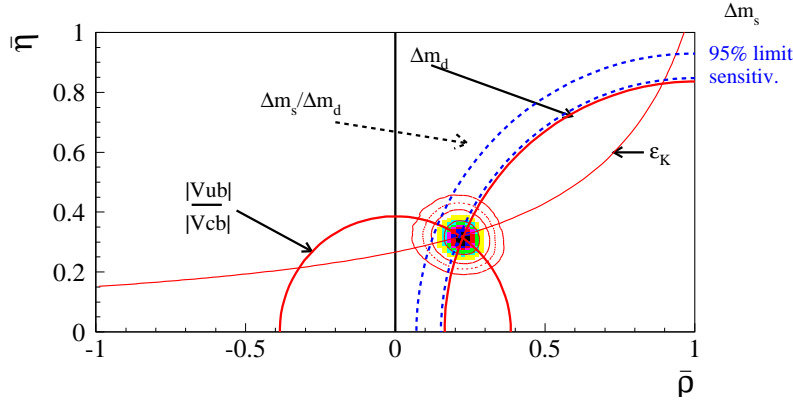


Fig. 6. Constraints on the (ϱ, η) vertex of the unitarity triangle [34]

which has three terms of a similar size. This relation can be visualized by a triangle in the complex plane, which is usually scaled by dividing its sides by $\mathbf{V}_{cb}^* \mathbf{V}_{cd}$. This aligns one side of the triangle along the real axis and makes its length equal to 1; the coordinates of the 3 vertices are then $(0, 0)$, $(1, 0)$ and (ϱ, η) . In the absence of CP violation ($\eta = 0$), this unitarity triangle would degenerate into a segment along the real axis.

The length of the sides and the angles (α, β, γ) of the unitarity triangle can be directly measured. In fact, we have already determined its sides from $\Gamma(b \rightarrow u)/\Gamma(b \rightarrow c)$ and B_d^0 - \bar{B}_d^0 mixing, and the position of the (ϱ, η) vertex has been further pinned down in Fig. 6 with ε_K . This gives [34]:

$$\varrho = 0.224 \pm 0.038, \quad \eta = 0.317 \pm 0.040, \quad \sin 2\beta = 0.698 \pm 0.066, \quad (25)$$

where $\beta \equiv -\arg(\mathbf{V}_{cd} \mathbf{V}_{cb}^* / \mathbf{V}_{td} \mathbf{V}_{tb}^*)$.

B^0 decays into CP self-conjugate final states provide independent ways to determine the angles [37]. The B^0 (or \bar{B}^0) can decay directly to the given final state f , or do it after the meson has been changed to its antiparticle via the mixing process. CP-violating effects can then result from the interference of these two contributions. The time-dependent CP-violating rate asymmetries contain direct information on the CKM parameters. The gold-plated decay mode is $B_d^0 \rightarrow J/\psi K_S$, which gives a clean measurement of β [38] without strong-interaction uncertainties, in good agreement with (25):

$$\sin 2\beta = 0.80 \pm 0.10. \quad (26)$$

Additional tests of the CKM matrix are underway. The B factories should accomplish an approximate determination of $\alpha \equiv -\arg(\mathbf{V}_{td} \mathbf{V}_{tb}^* / \mathbf{V}_{ud} \mathbf{V}_{ub}^*)$, from $B_d^0 \rightarrow \pi^+ \pi^-$, and many other interesting studies with B decays. Complementary and very valuable information could be also obtained from the kaon decay modes $K^\pm \rightarrow \pi^\pm \nu \bar{\nu}$, $K_L \rightarrow \pi^0 \nu \bar{\nu}$ and $K_L \rightarrow \pi^0 e^+ e^-$ [3,35].

6 Summary

The SM provides a beautiful theoretical framework which is able to accommodate all our present knowledge on electroweak and strong interactions. It is able to explain any single experimental fact and, in some cases, it has successfully passed very precise tests at the 0.1% to 1% level [5]. In spite of this impressive phenomenological success, the SM leaves too many unanswered questions to be considered as a complete description of the fundamental forces. We do not understand yet why fermions are replicated in three (and only three) nearly identical copies? Why the pattern of masses and mixings is what it is? Are the masses the only difference among the three families? What is the origin of the SM flavour structure? Which dynamics is responsible for the observed CP violation?

The fermionic flavour is the main source of arbitrary free parameters in the SM. The problem of fermion-mass generation is deeply related with the mechanism responsible for the electroweak SSB. Thus, the origin of these parameters lies in the most obscure part of the SM Lagrangian: the scalar sector. Clearly, the dynamics of flavour appears to be “terra incognita” which deserves a careful investigation.

The SM incorporates a mechanism to generate CP violation, through the single phase naturally occurring in the CKM matrix. Although the present laboratory experiments are well described, this mechanism is unable to explain the matter-antimatter asymmetry of our universe. A fundamental explanation of the origin of CP-violating phenomena is lacking.

Many interesting experimental signals are expected to be seen in the near future. Large surprises may well be discovered, probably giving the first hints of new physics and offering clues to the problems of mass generation, fermion mixing and family replication.

Acknowledgements

This work has been supported by MCYT, Spain (Grant FPA-2001-3031) and by the EU TMR network EURODAPHNE (Contract ERBFMX-CT98-0169).

References

1. S.L. Glashow: Nucl. Phys. **22**, 579 (1961). S. Weinberg: Phys. Rev. Lett. **19**, 1264 (1967). A. Salam: in *Elementary Particle Theory*, ed. by N. Svartholm (Almqvist and Wiksells, Stockholm 1969) p. 367. S.L. Glashow, J. Iliopoulos, L. Maiani: Phys. Rev. D **2**, 1285 (1970)
2. H. Fritzsch, M. Gell-Mann, H. Leutwyler: Phys. Lett. B **47**, 365 (1973)
3. A. Pich: ‘The Standard Model of Electroweak Interactions’, hep-ph/9412274; ‘Flavourdynamics’, hep-ph/9601202; ‘Rare Kaon Decays’, hep-ph/9610243; ‘Aspects of Quantum Chromodynamics’, hep-ph/0001118
4. A. Pich: Nucl. Phys. B (Proc. Suppl.) **66**, 456 (1998); **81**, 183 (2000); **98**, 385 (2001)
5. F. Gianotti: these proceedings

6. F. Jegerlehner: hep-ph/0104304. J.F. de Trocóniz, F.J. Ynduráin: Phys. Rev. D **65**, 093001, 093002 (2002). S. Narison: Phys. Lett. B **513**, 53 (2001); **526**, 414 (2002). A. Pich, J. Portolés: Phys. Rev. D **63**, 093005 (2001). M. Davier, A. Höcker: Phys. Lett. B **435**, 427 (1998). R. Alemany et al.: Eur. Phys. J. C **2**, 123 (1998)
7. H. Burkhardt, B. Pietrzyk: Phys. Lett. B **513**, 46 (2001); Eur. Phys. J. C **19**, 681 (2001). A.D. Martin et al.: Phys. Lett. B **492**, 69 (2000)
8. D.J. Gross, F. Wilczek: Phys. Rev. Lett. **30**, 1343 (1973). H.D. Politzer: Phys. Rev. Lett. **30**, 1346 (1973)
9. T. van Ritbergen et al.: Phys. Lett. B **400**, 379 (1997)
10. Particle Data Group: Eur. Phys. J. C **15**, 1 (2000); <http://pdg.lbl.gov/>
11. T. Kinoshita: Rep. Prog. Phys. **59**, 1459 (1996)
12. A. Czarnecki, W.J. Marciano: Phys. Rev. D **64**, 013014 (2001). J. Prades: hep-ph/0108192
13. H.N. Brown et al.: Phys. Rev. Lett. **86**, 2227 (2001)
14. M. Knecht, A. Nyffeler: Phys. Rev. D **65**, 073034 (2002). M. Knecht et al.: Phys. Rev. Lett. **88**, 071802 (2002). I. Blokland et al.: Phys. Rev. Lett. **82**, 071803 (2002). J. Bijnens et al.: Nucl. Phys. B **626**, 410 (2002). M. Hayakawa, T. Kinoshita: hep-ph/0112102. M.J. Ramsey-Musolf, M. Wise: hep-ph/0201297.
15. M. Hayakawa, T. Kinoshita: Phys. Rev. D **57**, 465 (1998). J. Bijnens et al.: Nucl. Phys. B **474**, 379 (1996); Phys. Rev. Lett. **75**, 1447, 3781 (1995)
16. M. Knecht et al.: hep-ph/0205102. S. Peris et al.: Phys. Lett. B **355**, 523 (1995). A. Czarnecki et al.: Phys. Rev. Lett. **76**, 3267 (1996); Phys. Rev. D **52**, 2619 (1995). T.V. Kukhto et al.: Nucl. Phys. B **371**, 567 (1992)
17. The LEP Collaborations ALEPH, DELPHI, L3, OPAL, the LEP Electroweak Working Group and the SLD Heavy Flavour Group: LEPEWWG/2002-01
18. P. Hernández: these proceedings
19. N. Cabibbo: Phys. Rev. Lett. **10**, 531 (1963)
20. M. Kobayashi and T. Maskawa: Progr. Theor. Phys. **42**, 652 (1973)
21. M. Artuso, E. Barberio: hep-ph/0205163
22. CLEO: Phys. Rev. D **61**, 052001 (2000)
23. LEP Heavy Flavour Steering Group: <http://lephfs.web.cern.ch/LEPHFS/>
24. CLEO: hep-ex/0202019
25. CDF: Phys. Rev. Lett. **86**, 3233 (2001)
26. L. Wolfenstein: Phys. Rev. Lett. **51**, 1945 (1983)
27. M. Ciuchini et al.: JHEP **0107**, 013 (2001)
28. K. Hagiwara, S. Narison, D. Nomura: hep-ph/0205092. A. Pich, J. Prades: Phys. Lett. B **346**, 342 (1995). A. Pich: Phys. Lett. B **206**, 322 (1988)
29. KTeV: Phys. Rev. Lett. **88**, 181601 (2002)
30. NA48: Eur. Phys. J. C **22**, 231 (2001); Phys. Lett. B **465**, 1999 (335)
31. NA31: Phys. Lett. B **317**, 1993 (233); **206**, 169 (1988)
32. R. Kessler: hep-ex/0110020; KTeV: Phys. Rev. Lett. **83**, 1999 (22)
33. E731: Phys. Rev. Lett. **70**, 1993 (1203)
34. ALEPH, CDF, DELPHI, L3, OPAL, SLD, hep-ex/0112028. F. Parodi, A. Stocchi: CKM Workshop (CERN, February 2002)
35. A.J. Buras: hep-ph/0101336
36. E. Pallante, A. Pich, I. Scimemi: Nucl. Phys. B **617**, 441 (2001). E. Pallante, A. Pich: Nucl. Phys. B **592**, 2000 (294); Phys. Rev. Lett. **84**, 2000 (2568)
37. A.B. Carter, A.I. Sanda: Phys. Rev. Lett. **45**, 952 (1980); Phys. Rev. D **23**, 1567 (1981). I.I. Bigi, A.I. Sanda: Nucl. Phys. B **193**, 85 (1981)
38. BABAR: hep-ex/0201020. BELLE: hep-ex/0202027. CDF: Phys. Rev. D **61**, 072005 (2000). ALEPH: Phys. Lett. B **492**, 259 (2000). OPAL: Eur. Phys. J. C **5**, 379 (1998)